University of
Sistan and Baluchestan

Iranian Journal of Archaeological Studies

Print ISSN: 2251-743X Online ISSN: 2676-2919

Archaeological Sciences
Research Centre

Archaeometric Investigation on the Grey Ware from Baluchestan, Iran: Intraregional Interactions in the Indo-Iranian Borderlands during the Late 4th–Early 3rd Millennia BCE

Mohamadreza Sheikhi[1], Yasin Sedghi[*,2], Nasir Eskandari[3], Mohammadamin Emami[4,5] and Mohammad Heydari[6]

[1] *Department of Architecture, Binalood University, Mashhad, Iran.*

[*]*Corresponding Author,* [2]*Department of Conservation of Cultural-historical Objects, Art University, Tehran, Iran.*
E- mail: sedghi.yasin@art.ac.ir

[3] *Department of Archaeology, University of Tehran, Tehran, Iran.*

[4] *Department of Conservation and Archaeometry, Art University of Isfahan, Isfahan, Iran.*

[5] *Plateforme Archéosciences, Université Bordeaux Montaigne, Bordeaux, France.*

[6] *General Direcotry of Cultural Heritage, Tourism and Handicrafts of Sistan and Baluchestan Province, Zahedan, Iran.*

Received: 12/ 01/ 2023; Received in Revised form: 16/ 04/ 2023; Accepted: 29/ 05/ 2023; Published: 20/ 06/ 2023

Abstract

The focus of this work is the archaeometric investigation of a high quality ceramic typical of the Indo-Iranian Borderlands in ca. 3300–2900 BCE. Variously labelled as "Emir Grey" and "Late Shahi Tump" ware, this fine grey ceramic is often considered an elite or prestige product on account of its very thin walls, fine fabric, and painted designs. In the present paper, thin-section petrography, XRD, and SEM-EDX analyses were carried out on a selection of pottery pieces from the burial contexts at the Chegerdak cemetery of Iranshahr (Baluchestan, Iran). The results shed new light on the production and circulation of the pottery. Most notably, it potentially extended the map of its production centers to western Iranian Baluchestan.

Keywords: Indo-Iranian Borderlands, Bronze Age, Chegerdak Cemetery, Archaeometry.

Article Type: Research Article

Introduction

The grey pottery designated as "Emir Grey" or "Late Shahi Tump" ware was first recorded by Stein at Shahi-Tump in 1928 (Stein 1931). C.C. Lamberg-Karlovsky and M. Tosi then identified the ware at Tepe Yahya and Shahr-i Sokhta in the 1960s and 1970s (Lamberg-Karlovsky & Tosi 1973). In the 1980s, R. Wright investigated and provided important details as to Emir Gray Ware (Wright 1984, 2002), including materials we can now link more precisely to the Late Shahi Tump (Mutin *et al,* 2017a) (Figure. 1). Since the famous survey program by A. Stein (1937) furnished the first data in the 1930s, establishing a reliable archaeological framework for the evolution of prehistoric cultures of Iranian Baluchestan has been an ongoing effort (e.g. see Lamberg-Karlovsky & Schmandt-Besserat 1977, de Cardi 1970, Sajjadi 2005, Mutin *et al*, 2017b). Production, chemical composition and distribution of this distinctive ceramic type have been the subjects of many publications (Wright 1984, Méry *et al*, 2013, Mutin *et al*, 2016, Mutin 2017a). In the last decade, B. Mutin conducted new comparative studies on the assemblages from Tepe Yahya, Shahr-i Sokhta, Kech-Makran, and

© The Author(s):

DOI: 10.22111/IJAS.2023.44984.1255
DOR: 20.1001.1.2251743.2023.13.1.7.8
Publisher: University of Sistan and Baluchestan

Iranian Baluchestan in order to refine its typology, chronology, and geographic distribution (Mutin, 2013: 84-90). More recently, Mutin and his colleagues have embarked on new instrumental neutron activation analysis of ceramics from 17 sites located hundreds of kilometers apart (e.g. Shahi-Tump and Miri Qalat in Southwestern Pakistan, Tepe Yahya in Kerman, Shahr-i Sokhta in Sistan and many sites in Iranian Baluchestan like Tepe Bampur and Khurab). Their results reinforced the picture of the Indo-Iranian Borderlands as a dynamic place for production and trade of high quality ceramics (Mutin 2017a).

The present paper addresses a small sample of the Late Shahi Tump pottery deriving from the plundered cemetery of Chegerdak, Iranshahr in southeastern Iran. This important Early Bronze Age (EBA) site in the plains of Jolgeh-ye Chah Hashem was identified in 2004, when Iranian archaeological authorities were informed of a new wave of large-scale clandestine excavations at the site. The ensuing rescue excavation by M. Heydari indicated that the graves mainly belonged to the late 4th–early 3rd millennium BCE (Heydari *et al*, 2015). The present study aims to explicate the industry and methods of pottery production at Chegerdak site using petrography (OPM), XRD, and SEM-EDX methods as well as their implications for our understanding of the dynamics of ceramic production and distribution in southeastern Iran during the EBA I (late 4th–early 3rd millennium BCE). To this end, 11 pieces of grey pottery from the Chegerdak cemetery, collected from the plundered graves during a systematic survey program, have been analyzed. Also, we will put the site of Chegerdak in the broader archaeological context of the Indo-Iranian Borderlands to gain an insight into the cross-regional interactions during the late 4th–early 3rd millennium BCE.

Context of Recovery and Chronology

In the EBA of southeastern Iran, important socio-cultural changes were going on, leading to the rise of early urbanization in this part of the Indo-Iranian Borderlands. Previous investigations in the well-known large urban centers of Shahr-i Sokhta, Shahdad and the valley of the Halil river

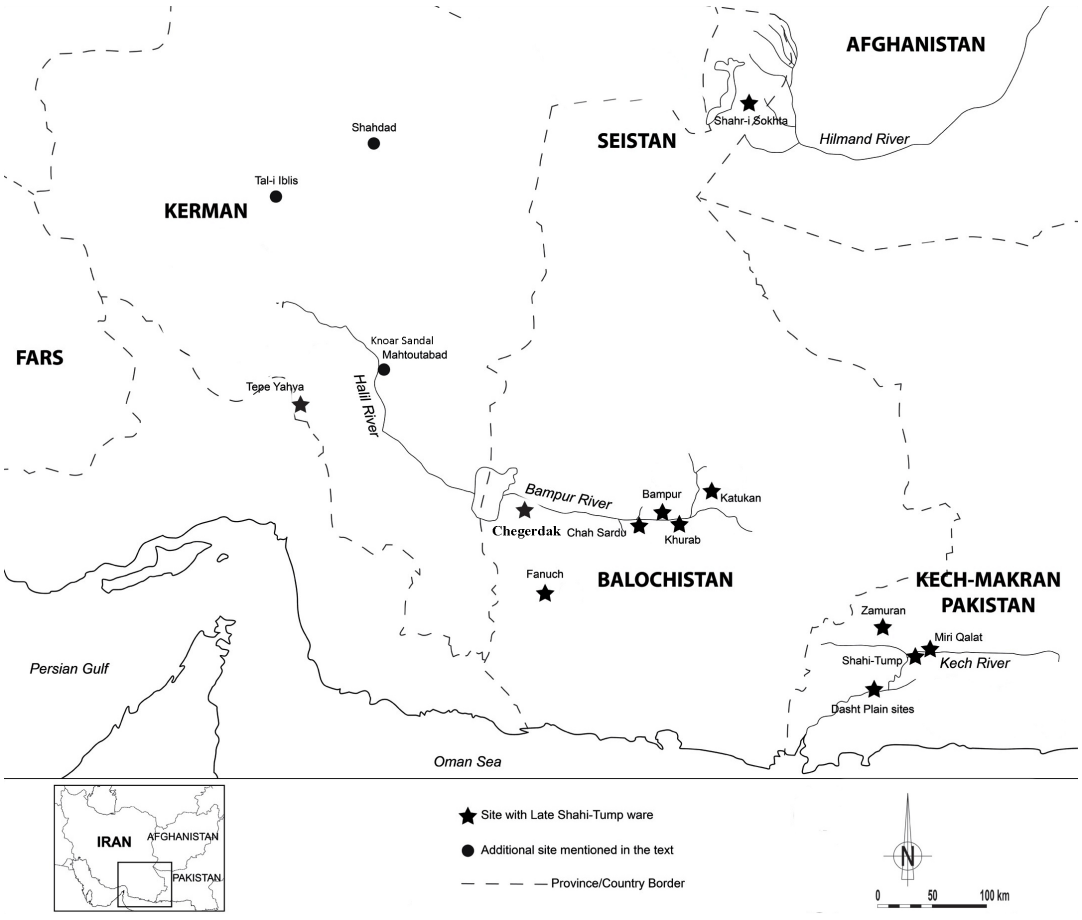


Figure. 1: *Map of southeastern Iran showing the location of the known sites with Grey Ware (Base map; After: Mutin et al 2017a, with some modifications)*

encompassing the region represented by the modern city of Jiroft have demonstrated that an urban florescence emerged in southeastern Iran, continued in the second quarter of the 3rd millennium BCE, and began to diminish by the end of the millennium (Eskandari 2019). The Baluchestan region (southeast Iran and southwest Pakistan) in the Indo-Iranian Borderlands was an important part of the regional urbanized landscape in the EBA, and thanks to its strategic position it controlled the trade networks linking southeast Iran and the Indus civilizations. Recent investigations at Chegerdak in the westernmost point of the Baluchestan region brought to light valuable information on the production and circulation of the grey ware tradition as well as the regional dynamics of southwestern Iran.

Located in Jolgeh-ye Chah Hashem District of Dalgan County, the ancient site of Chegerdak (27˚5'14" N, 59˚7'8" E) is 10 km northeast of the Chegerdak village and 200 km west of the Iranshahr city (Figure. 2). Geologically, the area lies between the northern fringes of the Upper Flysch Zone of eastern Iran (Falcon 1974; McCall & Kidd 1982; McCall 2002) and the more recent volcanic formation of Kuh-e Bazman (Figure. 3).

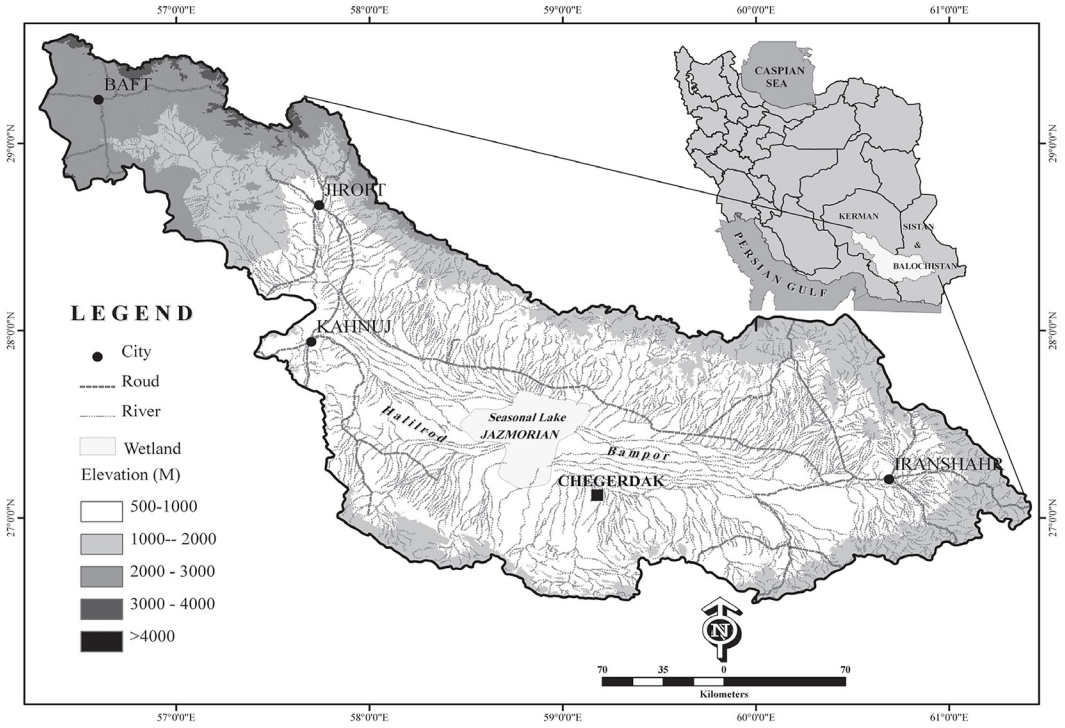


Figure. 2: *Map showing location of the archaeological site of Chegerdak in Iranian Baluchestan (After: Heydari et al, 2015)*



Figure. 3: *General view of the looted cemetery at Chegerdak. The settlement mound is seen in the background (Photo by M. Vidale)*

The ancient site of Chegerdak consists of a hill and two cemeteries dating to the EBA of Baluchestan. A detailed study on the collections of surface finds from the plundered graves of Chegerdak was published by a joint Iranian-Italian archaeological team, indicating that the site contains burials from the late 4th to the late 3rd millennium BCE (Heydari *et al*, 2015). The fine grey ware, the focus of the current research, dates back to the late 4th–early 3rd millennium BCE (3300–2900 BCE). This dating is backed by new radiocarbon dates from the site of Varamin in the Jiroft plain (Eskandari *et al*, 2020, Eskandari *et al*, 2021) and the Proto-Elamite level (IVC) at Tepe Yahya (Mutin 2013), where the Varamin period ceramics comparable with those of the Chegerdak cemetery were found. In addition, the fine painted grey ware of Chegerdak is known from many sites in Kech-Makran, Pakistan, among them being Shahi Tump (period IIIA) and Miri Qalat (Besenval 2005; Didier & Mutin 2015).

Materials and Methods

Samples

Figure 4 presents the selected sample of grey ware from Chegerdak. The surface ceramics point to an EBA settlement characterized by three pottery types: grey, buff, and red wares. The ceramics reveal important cultural links with the contemporaneous cultures of the Halil Rud basin to the northwest, the Sistan plains to the northeast, and the Kech Makran valleys to the southeast (Heidari *et al*, 2015). In this research, we will only focus on the grey ware that forms the bulk of the collection, and was described over 50 years ago in the following terms (Tosi 1970):

"[...] the grey ceramics [...] are related to mature stages of the process of urbanization that had the Helmand Basin as its centre, and spread into the valleys of Baluchestan, influencing a whole series of cultural centres that had been settled bit by bit along the perennial watercourses".

All the selected sherds are wheel-made, range from dark to light gray in color, and exhibit a thin fabric albeit with light variations in thickness (Table. 1). The specimens were coded by the initial of the site's name (CH) followed by a serial number from 1 to 11. Of these, nos. 1 to 8 represent sherds of the grey ware, while nos. 9 to 11 are complete bowls (Figures. 4, 5).

Methods

First, petrological and petrographical studies were carried out through preparing thin-sections and their observation via polarized light microscopy (OPM), using a James Swift polarized binocular microscope made in England at 4x and 10x magnifications. The purpose of petrographic experiments is to identify the mineralogical constituents of individual ceramic pieces and the difference in their mineralogical-chemical compositions, to determine the firing temperature based on the existing minerals, and finally, to provenance the raw materials used in their production (Roux 2011; Ceccarelli & Petrie 2018). Related experiments were performed at the Mineralogy and Petrography Laboratory of the Research Center for Conservation in Tehran.

SEM-EDX method was applied to examine micro-chemistry and micro-texture of the pottery matrix. Thus, the chemical-mineralogical characterization of the matrix and additives as well as vitrification stage of the pottery were studied. The samples were

Table. 1: *Specifications of the pottery sample considered in this study*

Sample Name	Color of motifs	Thickness (mm)	Type	Location of Motifs
CH1	Brown	3	Rim	Interior and exterior
CH2	Brown	2–3	Rim	Exterior
CH3	Brown	4	Body	Interior and exterior
CH4	Brown	5	Rim	Interior and exterior
CH5	Brown-Red	3–2	Rim	Interior and exterior
CH6	Brown-Red	5	Body	Interior and exterior
CH7	Black- Dark Brown	4	Rim	Interior and exterior
CH8	Dark Brown	4	Rim	Interior and exterior
CH9	Dark Brown	4	Complete bowl	Interior and exterior
CH10	Black	4	Complete bowl	Interior and exterior
CH11	-	5	Complete bowl	-

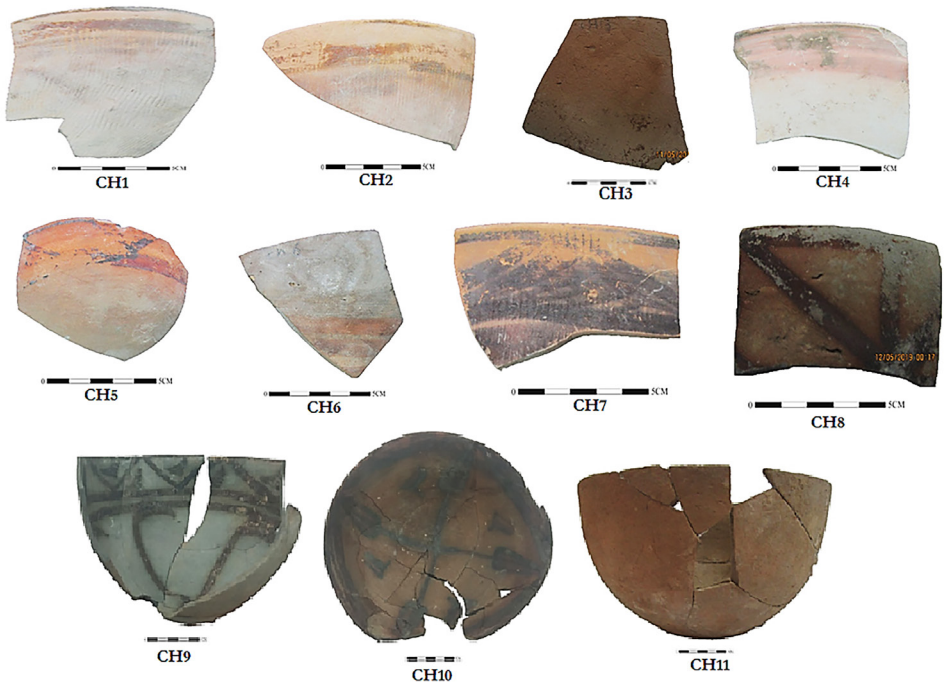


Figure. 4: *The selected specimens of the grey pottery from the Chegerdak cemetery*

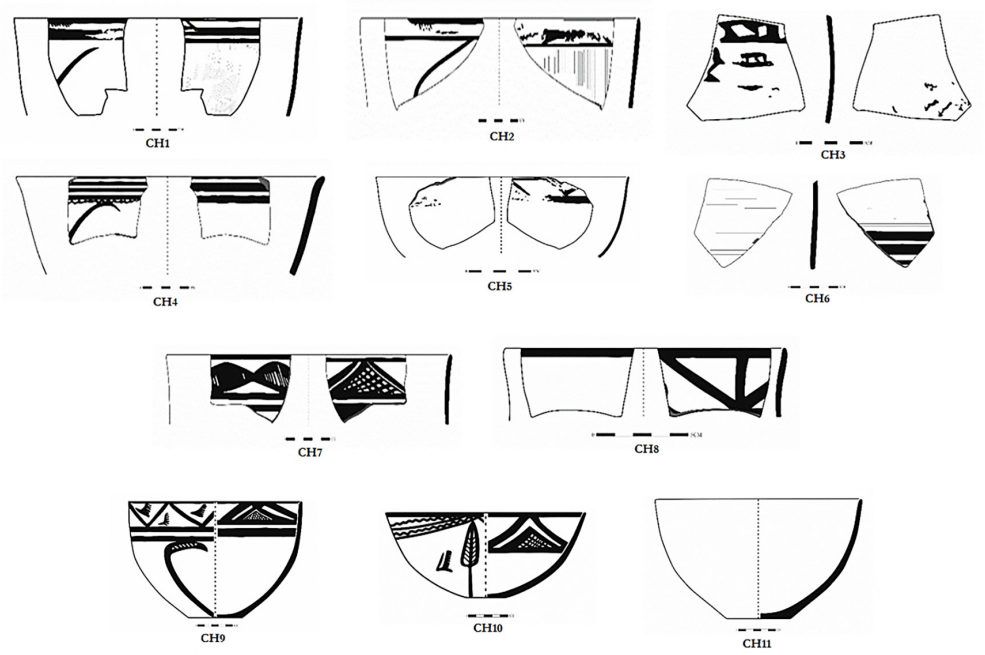


Figure. 5: *Drawings of the selected potteries, the Chegerdak cemetery*

analyzed as fractured pieces of the sherds. Also, in three cases (i.e. CH4, CH7, CH10) the paints used for the surface decorations were also sampled and characterized. To analyze the microstructure and chemical composition of the samples, a TESCAN MIRA3 FEG-SEM® SEM-EDX device was used. This analytical platform efficiently combines SEM imaging with elemental composition analysis in a single Essence™ software. The device is equipped with Fielmann field emission and works in both high and down vacuum operations. The resolution is set to 1nm and its magnification power is 1µm by applying 30KV voltage. In addition, the device is equipped with EDX INCAx-Sight (UK) which is suitable for qualitative and quantitative analysis of micro chemical composition. The precise

calibration feature (size) needs to be used for calibrating at a definite magnification. For essential calibration with a stable SEM, beam has to be correctly saturated on for at least 30-60 minutes. Calibration was done at a specific working distance and settings. These experiment were carried out at the Razi Metallurgical Laboratory in Tehran.

XRPD was applied to detect – qualitatively – the crystalline phases and the presence/absence of minute crystalline phases, detection of which are beyond the resolution of a polarization microscope. Samples were prepared from 0.5g of homogenized powders taken from the sherds. They were analyzed with the Brunker-D8 Diffractometer® (Made in Canada; X-ray producing tube lamp is made of copper (Cu) with 40KV potential difference and 30mA current intensity). XRPD was achieved on samples from (2θ=10°-60°). X'Pert HighScore Plus®-2008 ver. (2.2.c) program was used for XRD characterization throughout the study with a match function ratio of I/I0 (Emami 2020; Eramo 2020). All the related analyses were conducted at the Beam Gostar Taban Laboratory, and all the authors were responsible for the analytical procedure.

Results

Thin-Section Petrography

In order to facilitate the achievement of petrography outcomes (Freestone 1995), the results of this analysis are given in Table 2. This table is based on the petrography of the samples. In the first row, the components of the samples are presented, and in the first column the name and number of each sample are given separately (Freestone 1995; Peterson 2009).

Sample CH1: This sherd is in a fine fabric less than 2mm in thickness. The non-carbonate clay paste is accompanied by fine quartz pieces and iron oxide. Quartz is the most abundant ingredient in the paste, making up about 10% of the sample volume. This mineral is in fine-grained form, single crystal with angled to semi-rounded edge, and shows a light color under the microscope (see also Quinn 2009). Iron oxide is brown to dark in color and has a limited abundance in the paste. The size of the components does not exceed 20µ. The paste is quite homogeneous and contains limited voids.

Sample CH2: This is similar in composition to Sample CH1. Fine quartz pieces and iron oxide occurs within the non-carbonate clay paste, and quartz is again the dominant component at about 10%. The latter mineral is fine-grained, single-crystal with an angled to semi- rounded edge, and a light color can be seen under a microscope. Iron oxide is brown to dark in color and has a limited frequency in the paste. The components does not exceed 20µ in size. The highly homogenous paste shows only scarce voids.

Sample CH3: Unlike the previous two samples, here the paste is rather heterogeneous. Quartz is again the major constituent at 10%, and the dark clay fragments (grogs) used as filler account roughly for another 3% of the sample volume. The presence

Table. 2: *Results of petrography study of the grey pottery from the Chegerdak cemetery*

Number of Sample	Quartz phenocrysts	Quartz polycrystalline	Plagioclase	Fe-oxid	Amphibole &Pyroxene	Calcite	Grog	Mica	Texture
CH1	+++	+	-	+++	-	-	-	-	Silty
CH2	+++	+	-	+++	-	-	-	-	Silty
CH3	+++	+	-	+++	+	++	++	-	Silty
CH4	+++	+	-	+++	-	-	-	-	Silty
CH5	+++	+	-	+++	-	-	-	-	Silty
CH6	+++	+	++	+++	++	-	-	++	Silty
CH7	+++	+	-	+++	-	-	+	-	Silty
CH8	+++	+	-	+++	-	-	-	-	Silty
CH9	+++	+	-	+++	-	-	++	-	Silty
CH10	+++	+	-	+++	+	-	-	++	Silty
CH11	+++	+	-	+++	-	-	-	-	Silty

"+++" = high; "++" = medium; "+" = low; "–" = non-existent

of a small calcite component indicates a firing temperature below 800°C. Among other detected components was a limited amount of pyroxene.

Sample CH4: Characterized by a completely homogeneous paste, in this sample quartz particles occur in a very limited frequency as temper or filler.

Sample CH5: It features a composition similar to CH1 and CH2, with a non-carbonated clay paste containing small components of quartz and iron oxide. Quartz is typically the dominant ingredient, comprising about 10%–15% of the sample volume. This fine-grained, single-crystal mineral with an angled to semi-rounded edges appeared light colored under the microscope. The brown to dark iron oxide component showed a limited frequency in the paste. The size of the components did not exceed 20µ in this completely homogeneous paste with rather infrequent voids.

Sample CH6: This sherd revealed a composition completely at odds with the rest of the sample. A part from quartz, here were detected high amounts of phyllosilicate (mica), plagioclase, pyroxene and amphibole minerals, which were absent in the other samples. As these minerals are formed in igneous rocks, fragments of related rocks were seemingly added as temper (filler). Pyroxenes (simple chain silicates) are actually iron silicate, magnesium, and calcium that form at a temperature of at least 980°C (Riederer 2004). Due to the presence of igneous rocks in the northern and northeastern parts of the Jazmourian plate, the origin of this sample is probably completely different from the remaining samples.

Sample CH7: In this sample, quartz at a frequency of 5% is the most dominant component of the paste. Dark clay fragments (grogs) were used as filler and made up about 2% of the whole sample volume. Only limited voids were detected in the homogeneous paste (see also Quinn 2009).

Sample CH8: With its small contents of quartz and iron oxide, this sample paralleled Samples CH1, CH2 and CH5 in composition, which consisted of a non-carbonate clay paste. The most abundant quartz component made up about 5% of the sample volume. The mineral was fine-grained, single-crystal with an angled to semi-rounded edge and a light color under the microscope. Iron oxide was brown to dark in color and occurred in a limited frequency in the paste. This completely homogeneous paste contained only limited voids, and its components did not exceed 20µ in dimensions.

Sample CH9: This sherd proved to match Sample CH7 in terms of components. In this sample, quartz minerals were observed in the two forms of microcrystalline and macro crystalline, and had the highest abundance compared to all the other existing minerals. There were detected almost moderate amounts of grog fragments. As mentioned, this sample, like CH7, featured limited voids, and a homogeneous paste.

Sample CH10: As with the other samples, the homogeneous microcrystalline texture of this specimen contained a very high amount of microcrystalline quartz. Iron oxide and mica particles were also present.

Sample CH11: In the micrograph of this sample, microcrystalline quartz fragments and, to a lesser extent, large crystalline quartz are attestable. The microcrystalline quartz shows a much higher frequency than the other components. Like the entire sample, it has a homogeneous microcrystalline (silty) texture (Figure. 6).

SEM-EDX

This part of the study is devoted to microscopic and elemental analyses of the study sample using the SEM-EDX method (for details see Tite *et al*,1982). Given the close correspondence revealed between the samples in the thin-section petrography outlined above, only 3 samples, namely CH2, CH6 and CH8, were selected for SEM-EDX analysis. Micrographs were prepared from the petrographic thin-sections at different magnifications (Figures .5 & 7). Also, in some of the available points, including the matrix, grains and observed minerals, the EDX analysis has been performed in a point by point manner to identify their chemical composition and the EDX spectrum as an example (see Table . 3). Microscopic images show a sintered and semi-vitrified texture along with the secondary clays in the pottery, so that no porosity and cavities from improper hollowing and kneading are detectable (see also Maniatis & Tite 1981; Tite *et al*, 1982). Given the generally molten clay minerals and the formation of secondary minerals, such minerals are not readily identifiable. However, the melting occurred partially and some un-melted quartz were still remained. Concentrated and cemented texture and the paucity of voids observed in petrographic and microscopic experiments were also confirmed by the SEM images, so it is safe to assume that the potter had used suitable fine-grained minerals when

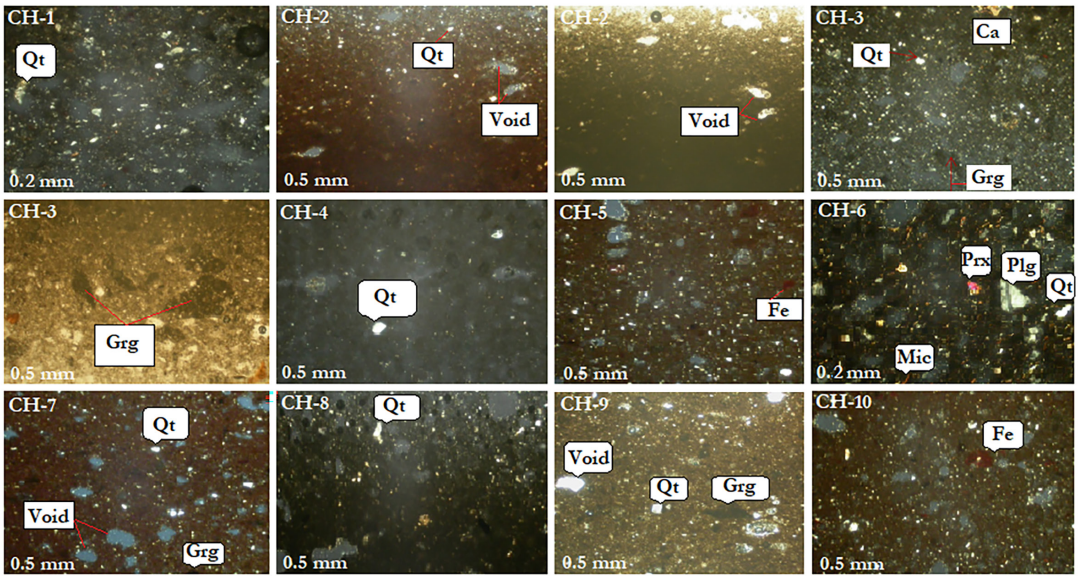


Figure. 6: *Photomicrograph of Sample (CH1), XPL light, 2.7mm field of view, silty texture, quartz, quartz mineral can be seen abundantly in the paste. Photomicrograph of Sample (CH2), XPL light, 2.7 mm field of view, silty texture, quartz mineral in the paste. Photomicrograph of Sample (CH2), PPL light, field of view length 2.7 mm, is the same as CH-8 in polarized light. In this light, the empty space is light in color. Photomicrograph of Sample (CH3), XPL light, 2.7 mm field of view, silty texture, quartz mineral with calcite and grog fragments are the main components of this sample. Photomicrograph of Sample (CH3), PPL light, field of view length 2.7 mm, is the same as CH-10 in polarized light. In this image, the grog parts are clearly visible. Photomicrograph of Sample (CH4), XPL light, 2.7 mm field of view, silty texture, completely homogeneous paste and the presence of a very limited number of quartz minerals in the paste. Photomicrograph of Sample (CH5), XPL light, field of view length 2.7 mm, silty texture, quartz mineral with iron oxide in the paste. Photomicrograph of Sample (CH6), XPL light, 2.7mm field of views, silty texture, quartz mineral with pyroxene, plagioclase and mica are among the constituents of the paste. Photomicrograph of Sample (CH7), XPL light, 2.7mm field of view, silty texture, quartz mineral with dark grog parts in the center of the image. Photomicrograph of Sample (CH8), XPL light, 2.7 mm field of view, silty texture, quartz mineral in the paste. Photomicrograph of Sample (CH9), XPL light, 2.7 mm field of view, silty texture, dark and scattered grog pieces can be seen in the paste. Photomicrograph of Sample (CH10), XPL light, 2.7mm field of view, abundant parts and small quartz can be seen in the paste.*

preparing the paste. In micrographs CH2-A, CH6-D and CH8-F in Figure 7, taken from semi-rounded silica phase, siliceous materials each respectively at 53.22, 72.56 and 100 weight percentiles, have been detected. The identified oxides also show the siliceous texture of the pottery so that the calcium content is very low and limited. Only in a single sample, CH8-E, it showed the percentile weight of 9.83, and the remaining samples contained only a very small amount of calcium. Quartz crystals reveal obvious cracks either as a result of crushing and grinding as part of temper preparation process or from a thermal pressure. Pottery with a quartz-rich matrix may crack due to quartz expansion at 573°C (Figure. 7, CH8-F), a possible causes of which is thermal damage during firing of pottery bodies (Tite *et al*, 1982; Emami *et al*, 2008) (Figure. 7; Table. 3).

EDX analysis was performed on Samples CH4, CH7 and CH10 with different color spectra to characterize the pigments applied by local prehistoric potters. The EDX analysis was taken point by point from the surface of the point on the pottery (Table. 4). In the preparation of pigments to be used in painted decorations on prehistoric pottery, iron oxides, often in the form of red or hematite, and magnetite as well as manganese oxide were generally employed to obtain dark and black colors, evidence of which have been identified in many recent studies (Čiuladienė *et al*, 2018; Mioč *et al*, 2004; Goodall *et al*, 2009; Afifi 2011; Sedghi *et al*, 2022). In the paints applied to the surface, the most common elements are silica, aluminum, iron and manganese. As X-ray penetrates into the inner layers of the pottery body, elements related to the

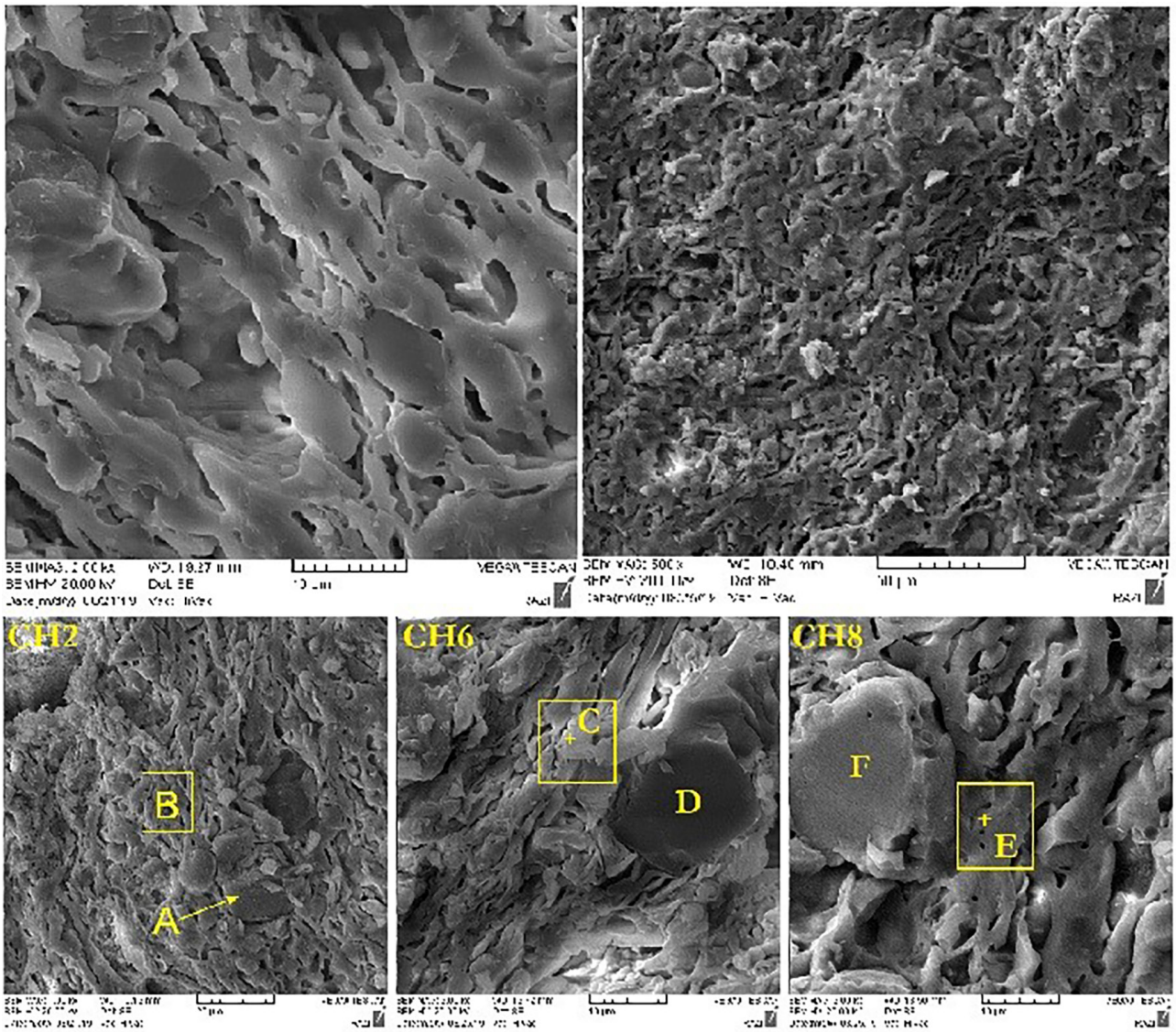


Figure. 7: *SEM images of Samples CH2, CH6 and CH8 showing the points where the thin-section was observed by EDX point analysis (After: Razi Metallurgical Laboratory, Tehran,Iran)*

Table. 3: *Results of chemical composition in SEM images (EDX analysis)*

Formula	CH2-A	CH2-B	CH6-C	CH6-D	CH8-E	CH8-F
Na2O	-	0.21	0.75	2.28	-	-
MgO	-	7.53	7.57	-	4.03	-
Al2O3	16.98	18.98	20.83	20.10	18.30	-
SiO2	53.22	53.36	48.05	72.56	54.10	100
K2O	26.22	4.78	5.29	1.05	4.05	-
CaO	1.67	0.71	0.91	1.40	9.83	-
FeO	1.91	14.39	16.56	2.49	9.66	-

Table. 4: Elements identified in the paints applied as decorative patterns to the samples.

Element	CH4	CH7	CH10
Oxygen	46.95	29.05	45.46
Sodium	1.20	-	4.65
Magnesium	1.21	1.45	1.60
Aluminium	11.66	3.61	6.54
Silicon	21.95	11.81	15.93
Sulfur	-	-	5.02
Chlorine	0.43	-	1.49
Potassium	1.58	0.87	1.07
Calcium	6.64	3.45	2.78
Titanium	1.40	0.56	-
Manganese	-	13.76	-
Iron	6.99	35.44	15.46
COLOR	Red	BLACK	BROWN

body's structure also become observable. However, the most important elements that can be related to the existing pigments are iron and manganese elements. The highest iron content were recorded for Sample CH7 at about 35.44% (weight percentage) and Sample CH10 at 15.45%, while the lowest amount, 6.99%, was detected in Sample CH4. On the other hand, Sample CH7 contained 13.76% of manganese element, which was otherwise undetected in the rest of the sample. Iron oxides were generally the most widely used colorant in antiquity. Iron oxide pigments range from dark yellow to red, crimson and brown. Its color base initially depends on the mineral's hydration level and also on the particles' size, shape and combination with other minerals. Anhydration of iron oxides, such as Fe_2O_3, will give purple-red to reddish-brown undertones. Hydration of iron oxides ($Fe_2O_3.NH_2O$) will make the color change to warm red and yellow. Manganese oxides are also important constituents of the pigment group, ranging from yellowish brown to black. These pigments have been used to decorate many pottery from prehistoric times. In light of the results of the analysis, the potters at Chegerdak clearly used iron-based minerals such as red ocher and hematite to decorate the red painted motifs and a combination of iron and manganese-based minerals for the dark and black patterns. The paints had become almost unstable during the post-depositional period and could be easily flicked away from the surface.

X- Ray Diffraction (XRD)

For crystallographic studies, Samples CH1, CH3, CH6 and CH7 were subjected to X-ray diffraction analysis by powder method (for details, see Roux 2011). The phases identified in this analysis are outlined in Table 5.To prevent duplication, only the XRD spectrum of Sample CH3 is given. Quartz is one of the most important identified phases. Clearly detectible in microscopic and chemical analyses, this phase also confirms the siliceous texture of the pottery. A silica-rich texture identified in all the analyses was confirmed here as well. This phase represents one of the primary phases identified here. Anorthite is another phase found to be present in the entire samples. Anorthite is a secondary, high-temperature phase in the feldspar group that will be stable to a temperature range of 930°C. Therefore, given its presence in the considered samples, their firing at higher temperature ranges is plausible. This means that the pottery in question has reached this temperature range (see also Emami & Trettin 2010; Maggetti & Schwab 1982). The microcline phase has been identified in two samples, CH7 and CH1. This phase is related to potassium feldspars with triclinic crystallization system, which is found in many metamorphic and igneous rocks. Hematite phase is a further phase identified for the two samples CH1 and CH7. Ferrous phases of iron oxide were detected in the thin-section petrography of all the samples. Here, given the grey color of the respective samples, these phases can be related to the clay resource, because, as stated earlier, significant amounts of iron oxides were observed in all the analyses, whether petrographic or chemical, and they were most post likely present in the raw clay and cannot be attributed to a high firing temperature.

Because, the formation of high heat resistance iron oxides will occur under oxidation conditions and high temperature of the furnace, a fact openly at variance with the type of kiln atmosphere under which the considered pottery pieces were fired — the reducing atmosphere. (Figure.8)

fragments were used as temper or filler. The fabric is invariably silty or microcrystalline, wholly consisting of fine-grained components that measure below 0.5mm. Quartz is present in all the samples and represents the main constituent. It is often

Table. 5: *XRD results obtained from the studied samples.*

Sample	Quartz	Anorthite	Albite	Hematite	Augite	Muscovite	Illite
CH1	+	+	+	+	+	+	+
CH3	+	+	-	-	-	+	+
CH6	+	+	-	-	+	+	+
CH7	+	+	+	+	+	+	+
Formula ICSD Code	SiO_2 089277	$Ca(Al_2Si_2O_8)$ 022505	$NaAlSi_3O_8$ 090142	Fe_2O_3 022505	$CaMgO_6Si_2$ 085162	$Al_3H_2KO1_2Si_3$ 030297	$Al_4H_3KO1_2Si_2$ 090144

Qz=Quartz, An=Anorthite, Ab=Albite, Hem=Hematite, Mus=Muscovite, Ill=Illite

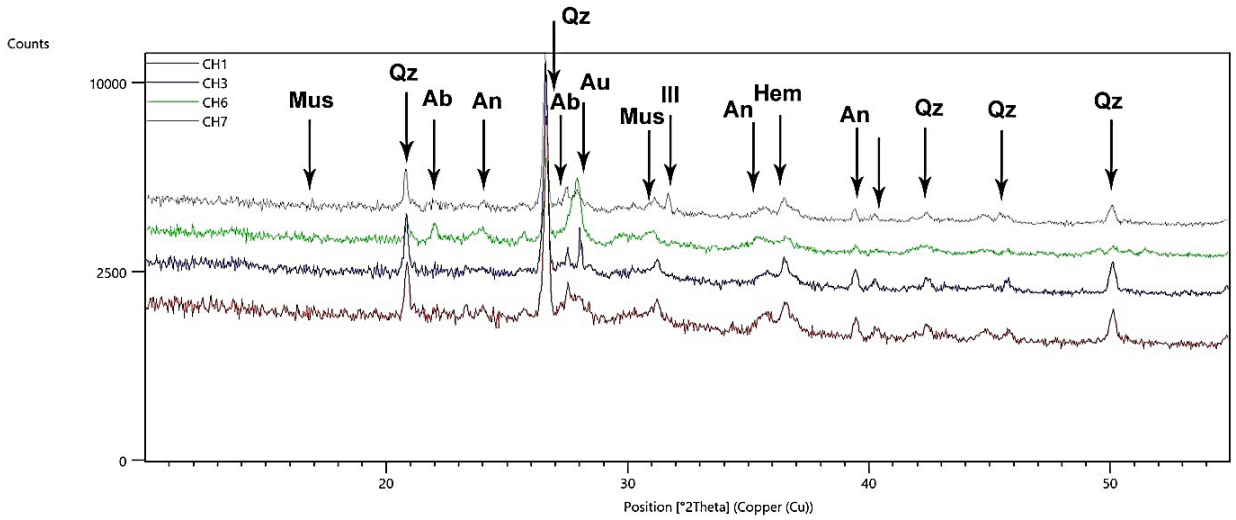


Figure. 8: *XRD diffractograms of the samples. (After: Beam-Gostar Taban Laboratory,Tehran,Iran)*

Discussion

Grey pottery is one of the most important finds from the less known area of Chegerdak in Baluchestan. Therefore, related finds have been analyzed and studied in this preliminary study using petrography, XRD, and SEM-EDX methods. In the first stage, the entire samples were subjected to petrography. In a petrography studies of pottery bodies, a central consideration involves the materials that were added to the paste (Ionescu *et al*, 2014). Archaeologists consider components larger than 0.1mm as additives or fillers (Roux 2011). In the considered samples, quartz and grog

seen in fine-grained, single-crystalline from with an angled to semi-rounded margins. Also present is polycrystalline quartz (multi-crystal), albeit in a very low frequency varying between 1% and 20% (see also Pincé *et al*, 2018; Núñez-Alarcón *et al*,2019). In Sample CH4, the quartz content, as the only constituent of the paste, is very limited, making up less than 1% of the sample volume. In pottery analysis, presence of primary calcite mineral is very significant as it acts as a thermometer. This mineral is burnt and vanished at firing temperatures of about 800°C (between 770°C–830°C depending on its composition), and thus will be absent from

the paste composition (Gliozzo 2020a; 2020b). Considering the regional geology that contains evidence of calcite mineral and carbonate rocks, the only plausible reason for the absence of calcite in the pottery paste is higher firing temperatures (see also Emami, 2020; Gliozzo 2020a; Abdolahzadeh *et al*, 2022). Among the entire considered samples, CH3 was the only sample to contain indications of calcite, thus firing of the original vessel at lower temperatures. The remaining samples were most plausibly exposed to temperatures of above 930°C judging from the results from their analysis. In Sample CH3, grog fragments were added as temper. These originally clay minerals are seen in a dark and relatively coarse color in the paste. Traces of grog fragments were otherwise detected only in Samples CH7 and CH10, and were absent from the other samples (also see Emami 2020). Sample CH6 stands out from the rest in terms of composition. Alongside quartz crystals, it contains phyllosilicate (mica), plagioclase, amphibole and pyroxene as well as iron oxide, minerals that occur in igneous rocks. The potter seemingly used igneous rock clasts as a tempering agent, and given the presence of igneous rocks in northern Jazmourian plate, this sample probably originated from that area. In this sample, quartz with a frequency of about 15%–20% is the dominant element, followed by mica (muscovite) at 5%, plagioclase at 3%, pyroxene, and amphibole at 1% along with iron oxide. The paste for all samples is homogeneous and non-carbonated, with relatively little voids (also see Hein and Kilikoglou 2018; Deng *et al,* 2019; Gianoncelli *et al*, 2020). In general, the pottery from the site petrographically falls into four classes. The first, and the most abundant, class is characterized by the domination of quartz and iron oxide as the paste components. Samples CH1, CH2, CH5, and CH8 fall into this category. The second class is represented by the three samples (CH3, CH7 and CH10) that in addition to quartz contain grog fragments as well (also see Mason and Cooper 1999). Made up of Samples CH4, CH9 and CH11, the third class is defined by a completely homogeneous fabric with a quartz content of less than 1%. Sample CH6 is the sole member of the fourth class that displays a completely different composition that contains igneous rock clasts or relevant sediments added as temper. Subsequently, SEM-EDX studies confirmed the petrographic analyses (also see Maniatis & Tite 1981; Tite *et al,* 1982). These analyses indicated a very dense, hard, and non-porous texture, suggesting that 5000 years ago the prehistoric potters of Chegerdak had adequate knowledge of clay kneading and processing to produce pottery vessels that lack in roughly any voids or indications of improper kneading. This point should be regarded among the foremost characteristics of the grey pottery in the region, especially in the southeast. On the other hand, the results show that the clay used for the paste was quite fitting, properly washed and free from any inclusions. Thus, the resultant vessels after firing became so resilient that could not be easily broken. This is clearly reflected in the vitrified texture of the pottery. Also in XRD phase analysis, high heat phases were detected (also see Emami 2020). It is very likely that high temperature kilns were responsible for their manufacture. On the other hand, during the fieldwork at the site, architectural remains from a pottery kiln, deformed potteries from overfiring, and wasters were discovered, attesting to the existing of local pottery craft at Chegerdak. The last stage of pottery production involved finishing and decorating the surface with a series of fine patterns. Elemental analyses demonstrated that the prehistoric artisans at Chegerdak used iron-based minerals such as hematite and red ocher to create red painted motifs and a combination of iron oxide and manganese based materials to produce black and dark paints.

Conclusions

The compositional analysis of the ceramic sample considered in this study indicated that, notwithstanding their similar composition, the EBA I (ca. 3300–2900 BCE) pottery pieces from the Chegerdak cemetery were manufactured using different techniques. Moreover, the results indicated the samples to have been fired in high temperatures. The existence of iron and manganese in the pigments forming the painted decorations evinces the presence of local pottery technology, production and trade at Chegerdak. In addition, the composition and structure of the local pottery bespeak the high level of expertise and knowledge of the potters who made a wide array of pottery pieces with diverse applications in the local community.

Archaeologically, the present archaeometric inquiry, in tandem with the previous chemical analyses on the distinctive grey ware, known as the Late Shahi Tump pottery, shows that the pottery was produced across the full extent of the

Baluchestan region since Chegerdak marks the westernmost production center of this pottery type in the EBA I according to the current state of our archaeological understanding. Furthermore, this ware was traded across Iranian Baluchestan, Kech-Makran (Southwestern Pakistan), the Halilrud cultural sphere of southern Iran, Iranian Sistan, and the Helmand region of southern Afghanistan. Circulation of this grey ware is a clear indication of dynamic intraregional interactions in the Indo-Iranian Borderlands at the dawn of early urbanization in this part of Southwest Asia.

Acknowledgment

The authors are grateful for permission granted by the Research Centre of Archaeology, Iranian Cultural Heritage Organisation, for the survey and sampling from the Chegerdak cemetery. Advice and support from Mrs Najmeh-Khatoon Miri, Mr Samad Elliyoun and other colleagues from University of Zabol is gratefully acknowledged. We are grateful for comments from two anonymous reviewers; any remaining errors are our own.

References

Abdolahzadeh, A; SP McPherron; DM Sandgathe ; TG Schurr; DI Olszewski & HL Dibble . 2022.Investigating variability in the frequency of fire use in the archaeological record of Late Pleistocene Europe. *Archaeological and Anthropological Sciences* 14(4):62. https://dx.doi.org/10.1007/s12520-022-01526-1

Afifi, H. A. 2011. Analytical Investigation of Pigments, Ground Layer and Media of Cartonnage Fragments from Greek Roman Period. *Mediterranean Archaeology & Archaeometry*, 11 (2). p. 91-98.

Besenval, R. 2005. Chronology of Protohistoric Kech-Makran. In C. Jarrige e V. Lefèvre (eds.) *South Asian Archaeology 2001*. Vol. 1, ERC, Paris, p. 1-9.

Ceccarelli, A. & C Petrie. 2018. Ceramic Analysis and the Indus Civilization. A Review. *Walking with the Unicorn, Social Organization and Material Culture in Ancient South Asia*, Edited by Dennys Frenez, Gregg M. Jamison, Randall W. Law, Massimo Vidale and Richard H. Meadow, Oxford OX2 7LG.

Čiuladienė, A.; A. Luckutė; J. Kiuberis & A . Kareiva. 2018. Investigation of the chemical composition of red pigments and binding media. *Chemija*, 29 (4). https://dx.doi.org/10.6001/chemija.v29i4.3840

De Cardi, B. 1970. *Excavations at Bampur, a Third Millennium Settlement in Persian Baluchestan,* 1966. Anthropological Papers of the American Museum of Natural History 51, no. 3. p. 233–355.

Deng, W; D. Backhouse; F. Kabir; R. Janani ; M. Bigharaz & A. Wardlow . 2019. An ancient technology could help deliver decarbonisation. *Glass International*. 42(7):47-9.

Didier, A & B. Mutin . 2015. The Kech-Makran region in Protohistoric Times. In U. Franke and E. Cortesi (eds.), Lost and Found. *Prehistoric Pottery Treasures from Baluchestan*, SMB, p. 297-333.

Emami, M. 2020. Production of Pottery from Esfandaghe and Jiroft, Iran, late 7th-early 3rd Millennium BCE. *Materials and Manufacturing Processes,* 35, 1446-1454. https://doi.org/10.1080/10426914.2020.1752919

Emami, S. M. A.; J. Volkmar & R. Trettin. 2008. Quantitative characterisation of damage mechanisms in ancient ceramics by quantitative X-ray powder diffraction, polarization microscopy, confocal laser scanning microscopy and non-contact mode atomic force microscopy. *Surface Engineering*. 24 (2): 129-137. https://doi.org/10.1179/174329408X298157.

Emami, S. M. & R . Trettin. 2010. Phase generating processes in ancient ceramic matrices through microstructure investigation with high resolution microscopy methods. *Journal of Advanced Microscopy Research*, 5(3), p. 181-189. https://dx.doi.org/10.1166/jamr.2010.1040

Eramo, G. 2020. Ceramic technology: how to recognize clay processing. *Archaeological and Anthropological Sciences*, 12. https://doi.org/10.1007/s12520-020-01132-z

Eskandari N. 2019. Regional patterns of Early Bronze Age urbanization in the southeastern Iran. New discoveries on the western fringe of Dasht-e Lut. In J.-W. Meyer, E. Vila, M. Mashkour, M. Casanova and R. Vallet (eds.) *The Iranian Plateau during the Bronze Age. Development of Urbanisation, Production and Trade*. Maison de l'Orient et de la Méditerranée, Jean Pouilloux, Lyon, 201-216.

Eskandari N.; F. Desset; M. Shafiee; M. Shahsavari; S. Anjamrouz; I. Caldana; A. Daneshi; A. Shahdadi & M. Vidale. 2021. Preliminary report on the survey of Hajjiabad-Varamin, a site of the Konar Sandal settlement network (Jiroft, Kerman, Iran), *IRAN* 59, p. 1-28. https://doi.org/10.1080/05786967.2021.1936595

Eskandari N.; M. Hessari; F. Desset; M. Vidale;M. Shahsavari & M. Shafiee. 2020. A late 4th to early 3rd millennium BCE grave in Hajjiabad-Varamin (Jiroft- south-eastern Iran): defining a new period of the Halil Rud valley prehistoric sequence. *Iranica Antiqua* 55. p. 1-48. https://doi.org/10.2143/IA.55.0.3289190

Falcon, N. L. 1974. Southern Iran: Zagros Mountains. *Geological Society, London, Special Publications*, 4, p. 199-211.

Freestone, I. C. 1995, The petrographic examination of ceramics, *American Journal of Archaeololgy* 99, 111-115.

Gianoncelli, A; S .Raneri ; S. Schoeder; T .Okbinoglu ; G. Barone & A. Santostefano . 2020.Synchrotron µ-XRF imaging and µ-XANES of black-glazed wares at the PUMA beamline: insights on technological markers for colonial productions. *Microchemical Journal*. 104629. https://doi.org/10.1016/j.microc.2020.104629

Gliozzo E. 2020a. Ceramic technology. How to reconstruct the firing process. *Archaeological and Anthropological Sciences* 12(11):260. https://doi.org/10.1007/s12520-020-01133-y

Gliozzo E. 2020b. Ceramics investigation: research questions and sampling criteria. *Archaeological and Anthropological Sciences*. 12(8):202. https://doi.org/10.1007/s12520-020-01128-9

Goodall, R. A.; J. Hall ; R. Viel & P. M.Fredericks. 2009. A spectroscopic investigation of pigment and ceramic samples from Copán, Honduras. *Archaeometry*, 51(1), p. 95-109. https://doi.org/10.1111/j.1475-4754.2007.00382.x

Hein, A & V. Kilikoglou . 2018. Modeling of the microstructure of ancient functional ceramics and assessment of their performance. *Procedia Structural Integrity*.10:219-26. https://doi.org/10.1016/j.prostr.2018.09.031

Heydari, M.; H. F. Nashli; E. Cortesi & M. Vidale.2015. A surface collection at Chegerdak, a Bronze Age center in the Jazmurian basin (South-Eastern Iran). *Paléorient*, vol. 41.2, p. 133-155. https://dx.doi.org/10.3406/paleo.2015.5680

Ionescu, C; V. Hoeck ; C. Gruian & V. Simon .2014. Insights into the EPR characteristics of heated carbonate-rich illitic clay. *Applied Clay Science* 97-98:138-45. https://doi.org/10.1016/j.clay.2014.05.023

Lamberg-Karlovsky, C. C. & D. Schmandt-Besserat.1977. An Evaluation of the Bampur, Khurab and Chah Husseini Collections in the Peabody Museum and Relations with Tepe Yahya. In *Mountains and lowlands: Essays in the Archaeology of Greater Mesopotamia, Bibliotheca Mesopotamica* 7, edited by L. Levine and T. C. Young, Jr., p. 113–134. Malibu: Undena.

Lamberg-Karlovsky, C. C. & M. Tosi. 1973. Shahr-i Sokhta and Tepe Yahya: Tracks on the Earliest History of the Iranian Plateau. *East and West* 23, p. 21-53.

Maggetti, M. & H. Schwab. 1982. Iron Age fine pottery from Châtillon-s-glâre and the Heuneburg. *Archaeometry,* 24(1), p. 21-36. https://doi.org/10.1111/j.1475-4754.1982.tb00644.x

Maniatis, Y. & M.S. Tite. 1981. Technological examination of Neolithic-Bronze Age pottery from central and southeast Europe and from the Near East, *Journal of Archaeological Science* 8, p. 59-76. https://doi.org/10.1016/0305-4403(81)90012-1

Mason, RB & L. Cooper . 1999. Grog, petrology, and early transcaucasians at Godin Tepe. *Iran*: 25-31. https://doi.org/10.2307/4299991

McCall, G.J.H. 2002. A summary of the geology of the Iranian Makran. In: Clift P.D., Kroon D., Gaedicke C. and Craig J. (eds.), *the Tectonic and Climatic Evolution of the Arabian Sea Region:* 147-204. London: The Geological Society (Geological Society, London, Special Publications 195, 1).

McCall, G.J.H. & R.G.W. Kidd . 1982. The Makran, Southeastern Iran: the anatomy of a convergent plate margin, active from the Cretaceous to the Present. In: Leggett J.K. (ed.), *Trench-Forearc Geology. Sedimentation and Tectonics on Modern and Ancient Active Plate Margins*: 387-397. Oxford, London: Blackwell Sci., The Geological Society (Geological Society, London, Special Publications 10).

Méry, S.; M. J. Blackman; A. Didier & R. Besenval.2013. A centre of production and diffusion for fine grey pottery in the third millennium: the pottery workshops of the Dasht Plain (Makran, Pakistan) and the Oman peninsula. *Archäologische Mitteilungen aus Iran und Turan* 45, p. 169-198.

Mioč, U. B.; P. Colomban; G. Sagon; M. Stojanović, & A. Rosić. 2004. Ochre decor and cinnabar residues in Neolithic pottery from Vinča, Serbia. *Journal of Raman Spectroscopy* 35(10), p. 843-846. https://doi.org/10.1002/jrs.1221

Mutin, B.; H. Moradi;H. Sarhaddi-Dadian; H. Fazeli Nashli & M. Soltani. 2017b. New Discoveries in the Bampur Valley (South-Eastern Iran) and Their Implications for the Understanding of Settlement Pattern in the Indo-Iranian Borderlands during the Chalcolithic Period. *Iran*, 55, 2, p. 1-21. https://doi.org/10.1080/05786967.2017.1356004

Mutin, B. 2013. T*he Proto-Elamite Settlement and its Neighbours*. Tepe Yahya Period IVC, American School of Prehistoric Research Monograph Series, Oxford and Oakville.

Mutin, B.; C. C. Lamberg-Karlovsky &L. Minc. 2016. Investigating ceramic production during the Proto-Elamite period at Tepe Yahya, southeastern Iran: Results of instrumental neutron activation analysis of periods IVC and IVB ceramics. *Journal of Archaeological Science: Reports,* 7, 849-862. https://doi.org/10.1016/j.jasrep.2016.02.019

Mutin, B; L.D. Minc; C.C. Lamberg-Karlovsky & M. Tosi. 2017a. Regional and long-distance exchange of an emblematic 'prestige' ceramic in the Indo-Iranian Borderlands. Results of Neutron Activation Analysis., *Paléorient*, vol. 43.1, p. 141-162. https://dx.doi.org/10.3406/paleo.2017.5755

Núñez-Alarcón, E; L.Puentes-Arguello & J. Barrios-López. 2019. Mineralogical characterization of an ancient pottery from the la Candelaria archaeological site, Santa Helena del Opón, Santander (Colombia). *Int Phys Med Rehab* J. 3(4):118-24. https://dx.doi.org/10.15406/mseij.2019.03.00101

Peterson, S. E. 2009. *Thin-section Petrography of Ceramic Material*s, Philadelphia, PA: INSTAP Academic Press.

Pincé, P; D. Braekmans ; N. Abdali ; E. De Pauw ; S, Amelirad & P. Vandenabeele . 2018. Development of ceramic production in the Kur River Basin (Fars, Iran) during the Neolithic. A compositional and technological approach using X-ray fluorescence spectroscopy and thin section petrography. *Archaeological and Anthropological Sciences* 11(4):1241-58. https://doi.org/10.1007/s12520-018-0598-6

Quinn, P. S., ed. 2009. *Interpreting Silent Artefacts: Petrographic Approaches to Archaeological Ceramics,* Oxford: Archaeopress.

Riederer, J. 2004. Thin Section Microscopy applied to the study of archaeological Ceramics. *Hyperfine Interactions* ,154,143-153.https://doi.org/10.1023/B:HYPE.0000032029.24557.b1

Roux, V. 2011. Anthropological interpretation of ceramic assemblages: foundations and implementations of technological analysis, in S. Scarcella, ed., '*Archaeological Ceramics: a Review of Current Research'*, Oxford: Archaeopress, pp. 80-88.

Sajjadi, S. M. S. 2005. *Bampur Tepe. The First Season of Excavations at Bampur Tepe*. Archaeological Report Monograph Series 6. Tehran: ICAR.

Sedghi, Y.; F. Sabouhi Sani; N. Eskandari & M. Emami. 2022. Beyond a Decoration; Mineralogical and Micro-structural Study of the Early Bronze Age "Life Cycle Jar" from Keshik Cemetery, Sistan and Balouchistan, Iran, Interdisciplinaria Archaeologica VIII, 1-12. https://doi.org/10.24916/iansa.2022.2.2

Tite, M. S.; I. C. Freestone; N. D. Meeks & M. Bimson. 1982 The use of scanning electron microscopy in the technological analysis of ancient ceramics, in J. S. Olin & A. D. Franklin, ed., '*Archaeological Ceramics*', Washington, D.C.: Smithsonian Institution Press, pp. 109-120.

Tosi, M. 1970. A Tomb from Damin and the Problem of the Bampur Sequence in the Third Millennium BCE. *East and West* 20, 1-2: 9-50.

Wright, R.P. 1984. *Technology, Style and Craft Specialization: Spheres of Interaction and Exchange in the Indo-Iranian Borderlands, Third Millennium BCE* (Ph.D. dissertation) Department of Anthropology, Harvard University.